CHIN. PHYS. LETT. Vol. 37, No. 11 (2020) 116201

Shear-Banding Evolution Dynamics during High Temperature Compression of Martensitic Ti-6Al-4V Alloy

Xue-Hua Zhang(张雪华)[1,2*], Rong Li(李荣)[3], Yong-Qing Zhao(赵永庆)[1,3*], and Wei-Dong Zeng(曾卫东)[1]

[1]*State Key Laboratory of Solidification Processing, Northwestern Polytechnical University, Xi'an 710072, China*
[2]*Western Metal Materials Co., LTD, Xi'an 710021, China*
[3]*Northwest Institute for Nonferrous Metal Research, Xi'an 710016, China*

(Received 4 July 2020; accepted 9 September 2020; published online 8 November 2020)

The isothermal compression dynamics of ternary Ti-6Al-4V alloy with initial martensitic structures were investigated in the high temperature range 1083–1173 K and moderate strain rate regime 0.01–10 s^{-1}. Shear banding was found to still dominate the deformation mechanism of this process, despite its nonadiabatic feature. The constitutive equation was derived with the aid of Zener–Hollomon parameter, which predicted the apparent activation energy as 534.39 kJ/mol. A combination of higher deformation temperature and lower strain rate suppressed the peak flow stress and promoted the evolution of shear bands. Both experiments and calculations demonstrated that a conspicuous temperature rise up to 83 K could be induced by severe plastic deformation. This facilitated the dynamic recrystallization of deformed martensites, as evidenced by the measured microhardness profiles across shear bands.

PACS: 62.20.F−, 62.20.−x, 81.40.Ef, 81.40.Lm DOI: 10.1088/0256-307X/37/11/116201

The formation of shear bands is a common physical phenomenon during the plastic deformation of numerous condensed matter systems.[1−8] This dynamic process is characterized by the drastic localization of shear strain and it results in the formation of a strip of seriously deformed zone. It is not only a classical topic of solid mechanics but has also become an intriguing subject for the interdisciplinary research in structural geology,[9,10] civil engineering[11] and materials science.[12] Tectonic explorations provided the most magnificent example of natural rock shear bands formed through the geological movements of earth's crust,[3,9,10] which extended over hundreds of kilometers. In the field of soil mechanics and civil engineering, the study about Coulomb-type shear bands of granular materials dates back to almost two and a half centuries ago.[13] An extreme case is the high explosive ignition of energetic materials by granular shear bands.[14] As for this kind of instable plastic flow at nanoscale and even atomistic dimension, there have been extensive investigations upon various advanced materials, including ferrous/nonferrous alloys,[1,15] bulk metallic glasses[2,4,5,8,12] and novel composites.[16,17]

Shear banding is the dominant deformation mechanism of metallic glasses because of the amorphous state of their microstructures.[2,5,18−20] In contrast, traditional crystalline metals and alloys display shear bands only when their strain rate, deformation temperature and pretreated status ensure an appropriate combined condition. The apparent physical mechanism is the dynamic balance between their strain hardening and thermal softening during tensile, compressive or impact deformation. This complicated process essentially involves the movements of voids and dislocations and even experiences the dynamic recovery and recrystallization of severely deformed crystalline materials. If the strain rate is sufficiently high to exceed 10^3 s^{-1}, just as in the projectile and explosion situations, then the so-called adiabatic shear bands are produced because the deformation induced heat cannot dissipate quickly enough to prevent a conspicuous temperature rise.

Owing to their great specific strength and excellent high temperature performances, titanium alloys become the important structural materials for aerospace technology. In particular, the most popular ternary Ti-6Al-4V alloy has found further applications also in chemical engineering, metallurgical industry and even medical instruments. This category of hexagonal closely packed alloys exhibits strong deformation resistance but weak thermal conductivity, and thus are prone to form shear bands. Although a large number of analytical and experimental studies have been accomplished to correlate shear band features with the mechanical properties of titanium alloys,[15,21−26] the underlying physical essence of shear banding dynamics still needs more elaborate explorations. The objec-

Supported by the National Natural Science Foundation of China (Grant No. 51471136), and the Fundamental Research Funds for Central Universities.
*Corresponding author. Email: zxhxyt@126.com; trc@c-nin.com
© 2020 Chinese Physical Society and IOP Publishing Ltd

tive of this Letter is to investigate the dynamic evolution mechanism of shear bands during the isothermal compression of Ti-6Al-4V alloy with initial martensite structures under moderate strain rate but elevated temperature conditions.

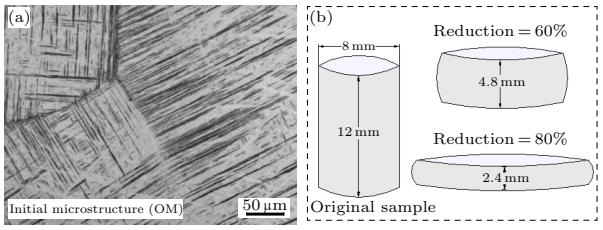

Fig. 1. Initial martensitic microstructures (a) and original and deformed sample shapes (b).

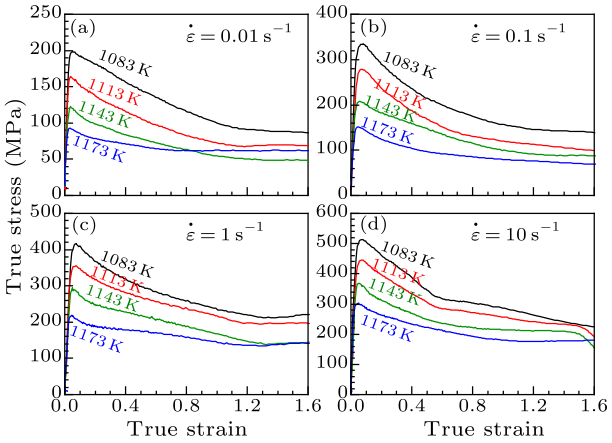

Fig. 2. True stress-true strain curves of Ti-6Al-4V alloy subject to isothermal compressions under various temperature and strain rates.

The experimental material was taken from an industrial Ti-6Al-4V alloy sheet produced by China Western Titanium Technologies Co. Ltd. Its chemical composition was (wt%): 6.16 Al, 4.17 V, 0.062 Fe, 0.15 O, 0.009 C, 0.003 N, 0.002 H and with the balance of Ti. It showed an α/β transition temperature of about 1253 K. The as-rolled alloy sheet was firstly β-solution treated at 1283 K for 30 min, and then subject to water quenching to obtain the martensitic microstructures, which were composed of long orthogonally distributed α' laths with an acicular morphology presented in Fig. 1(a). As illustrated in Fig. 1(b), the cylindrical compression samples had a diameter of 8 mm and a height of 12 mm. The uniaxial compression tests were conducted with a Gleebe-3800 thermomechanical simulator. Four deformation temperatures were predetermined as 1083, 1113, 1143 and 1173 K, respectively, while four strain rates were chosen as 0.01, 0.1, 1 and $10\,s^{-1}$. The samples were heated to the desired deformation temperatures at a heating rate of 10 K/s, held for 5 min to achieve thermal homogenization, then pressed to a height reduction of 60%(true strain $\varepsilon = 0.9$) and 80%($\varepsilon = 1.6$), and finally quenched by water to retain the deformed microstructures at high temperatures. A $PtRh_{10}$-Pt thermal couple with 0.3 mm wire diameter was attached to the midpoint of each sample surface to measure the temperature rise caused by compressive deformation. After the isothermal compression experiments, all the samples were sectioned along their vertical axes, polished and etched with a mixed solution of $HF:HNO_3:H_2O = 1:1:5$. Their deformed macroscopic structure and microstructural morphology were analyzed by Zeiss 40MAT optical microscope and Zeiss Supera 55 scanning electron microscope. Meanwhile, Vickers hardness was measured with an MMT-3 microhardness instrument, where the load of 500 gf (i.e., 4.9 N) and Dwell time of 10 s were employed.

The true stress-strain curves of Ti-6Al-4V alloy during isothermal compression tests are presented in Fig. 2. Obviously, these dynamic curves all exhibit a peak stress at very low strains, which is followed by an extensive flow softening stage. As seen in Fig. 3(a), the peak stress decreases with the enhancement of deformation temperature, but increases with the elevation of strain rate. Such a strain rate effect is actually concerned with dislocation movements, where the migrating velocity of dislocations increases with strain rate and thus leads to the rise of flow stress. In order to characterize the deformation dynamics properly, the constitutive equation is contrived with the aid of Zener–Hollomon parameter Z. For this purpose, the sine hyperbolic expression is applied to correlate the true stress σ and strain rate $\dot{\varepsilon}$ with deformation temperature T:[27,28]

$$Z = A[\sinh(\alpha\sigma)]^n = \dot{\varepsilon}\exp(Q/RT), \tag{1}$$

where R stands for the gas constant. The activation energy Q of plastic deformation together with the three material constants A, α and n is determined by the following coupled equations:

$$\alpha = \frac{d\ln\dot{\varepsilon}/d\sigma}{d\ln\dot{\varepsilon}/d\ln\sigma}, \tag{2}$$

$$Q = R\left\{\frac{\partial\ln\dot{\varepsilon}}{\partial\ln[\sinh(\alpha\sigma)]}\right\}_T\left\{\frac{\partial\ln[\sinh(\alpha\sigma)]}{\partial(1/T)}\right\}_{\dot{\varepsilon}}, \tag{3}$$

$$\ln Z = \ln A + n\ln[\sinh(\alpha\sigma)]\,. \tag{4}$$

According to the experimental results shown in Fig. 2, the activation energy Q of compressive deformation for martensitic Ti-6Al-4V alloy is derived to be 534.39 kJ/mol. This is similar to the Q value of 535 kJ/mol for the same alloy with initially lamellar microstructures,[24] while significantly higher than that of 472.57 kJ/mol for the case with originally equiaxed microstructures.[28] In a further comparison, this is also far beyond the grain boundary self-diffusion energy for α-Ti and β-Ti.[23] Judging from this respect, the dynamic recrystallization (DRX) of martensitic α' phase may have taken place in the isothermal

compression process. Meanwhile, the three material constants α, A and n for martensitic Ti-6Al-4V alloy have been determined to be $4.2 \times 10^{-3}\,\mathrm{MPa}^{-1}$, 4.45×10^{23} and 4.75, respectively. Finally, the constitutive equation of this alloy is obtained as follows:

$$\dot{\varepsilon} = 4.45 \times 10^{23} \left[\sinh\left(4.2 \times 10^{-3}\sigma\right)\right]^{4.75} \cdot \exp(-534.39/RT). \quad (5)$$

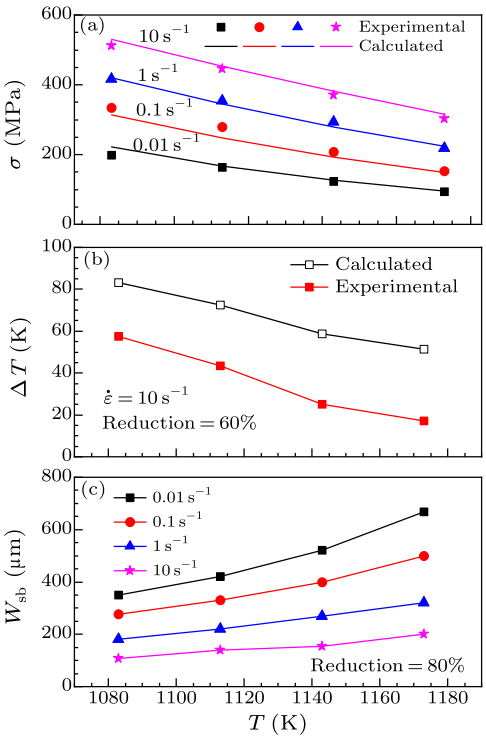

Fig. 3. Dynamic and physical characteristics of Ti-6Al-4V alloy subject to isothermal compression: (a) calculated and experimental flow stresses, (b) deformation-induced temperature rise, and (c) shear band width.

Figure 4 provides the typical structural morphologies of martensitic Ti-6Al-4V alloy after isothermal deformation. It is evident that all the compressed samples with 60% and 80% height reduction became drum-shaped, which was caused by the friction on contact surface accompanying their deformation processes. Usually, three different deformation zones were observed in most of these samples. The first zone is the shear band with severe plastic deformation, as indicated by A in Figs. 4(a) and 4(b). If the total amount of compressive strain is relatively small or the deformation temperature is comparatively lower, then two or one dead zones without apparent deformation will appear around the sample top and bottom ends in touch with the testing compressor surface, which are designated as C in Figs. 4(a) and 4(b). Between these two extreme zones A and C, there exists the third transition zone B of partial plastic deformation. As shown in Fig. 4(a), the shear bands formed under the smaller true strain $\varepsilon = 0.9$ are often located near the sample centers. When deformed at the lower temperature of 1083 K and the faster strain rate of $\dot{\varepsilon} = 10\,\mathrm{s}^{-1}$, the shear banding direction displays an angle of 45° to the compressing axis. If the deformation temperature is raised up to 1173 K and the strain rate is depressed down to $0.01\,\mathrm{s}^{-1}$, then the orientation of shear bands becomes nearly perpendicular to the compressive direction.

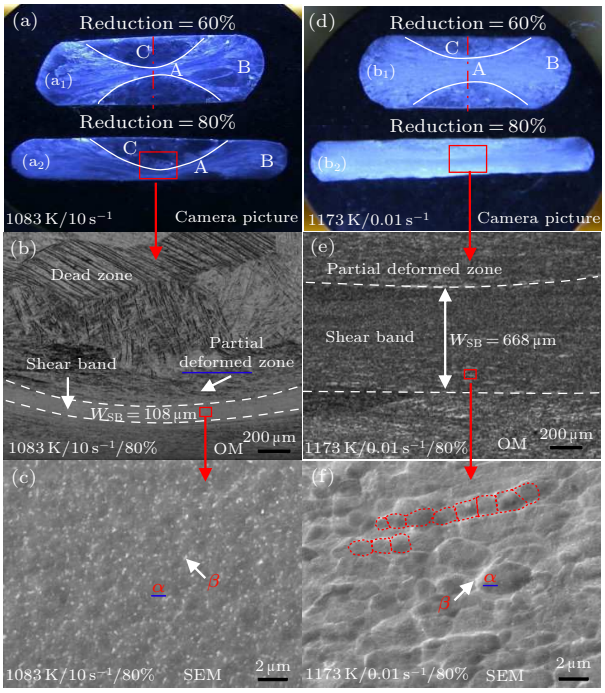

Fig. 4. Macrostructure and microstructure of isothermally compressed Ti-6Al-4V alloy samples: (a)–(c) deformed at 1083 K/10 s^{-1}, (d)–(f) deformed at 1173 K/0.01 s^{-1}.

It is revealed by experimental measurements that the width of shear band increases with the rise of deformation temperature but decreases with the acceleration of strain rate, as illustrated in Figs. 3(c), 4(c) and 4(d). The main reason for this is that the diffusion of grain boundaries is greatly enhanced with deformed temperature increasing, more martensites α' phase transformed into equiaxed grains, thus the width of shear band increases. Under the compressive condition of 1083 K temperature and 10 s^{-1} strain rate, the shear band width is only 108 μm in the case of 1.6 true strain. This increases up to 668 μm when the deformation temperature is elevated to 1173 K and the strain rate depressed to $0.01\,\mathrm{s}^{-1}$. In contrast, the enhancements of both deformation temperature and true strain consistently reduce the area of dead zone, which almost disappears under the temperature and strain conditions of 1173 K and 1.6. The internal microstructures of shear bands have transformed from the initial martensites α' phase of Fig. 1(a) into the refined equiaxed grains of α phase in Figs. 4(e) and 4(f), where some adjacent α grains display a necklace-like configuration. On the other hand, the dead zone C

mainly involves martensitic microstructures, whereas the transition zone B consists of remnant martensite needles and transformed α phase grains. Evidently, dynamic recovery and recrystallization have occurred within the shear bands and at least partially also inside the transition zones. Moreover, a larger true deformation strain is also found to promote the microstructural transitions. The average α phase grain size in shear band increases with elevated deformation temperature and reduced strain rate. When isothermally compressed under the condition of 1083 K and $10\,s^{-1}$, α phase grains showed an average size of 1 μm. This grain size became doubled once the deformation condition was changed into the higher temperature of 1173 K and the slower strain rate of $0.01\,s^{-1}$. Based upon a comprehensive consideration together with the dynamic features of stress-strain curves, it is inferred that the deformation induced temperature rise and the recrystallized structure globulation have brought about the flow softening in isothermal compression process.

The low thermal conductivity of Ti alloys is favorable to the evolution of shear banding. Although the predetermined moderate strain rate regime of 0.01–$10\,s^{-1}$ does not secure a thermodynamically adiabatic process, the experimental temperature and the deformation induced temperature rise coupled with the suitable time extension are potent enough to initiate the dynamic recovery and recrystallization of severely compressed crystalline microstructures within shear bands. At the relatively faster strain rate of $10\,s^{-1}$, it took only 0.12 s to perform the height reduction of 60%, which corresponded to a true strain of 0.9. Such an isothermal compression processing aroused a conspicuous temperature rise ΔT for the deformed sample. This important processing parameter was theoretically predicted by the equations[29,30]

$$\Delta T = \frac{\beta_0}{\rho C_V}\int_{\varepsilon_s}^{\varepsilon_e}\sigma d\varepsilon \approx \frac{\beta_0}{\rho C_V}\sum_{i=1}^{m} S_i, \tag{6}$$

$$S_i = \frac{1}{2}(\sigma_i + \sigma_{i+1})\Delta\varepsilon_i, \tag{7}$$

where β_0 is the fraction of plastic energy converted into heat, usually evaluated as 0.9. S_i represents the deformation energy per unit area and is determined by the stress-strain curves. For Ti-6Al-4V alloy, the density ρ equals $4440\,kg/m^3$, and the heat capacity C_V is 840 J/kg·K. A comparison between theoretical prediction and experimental result is provided in Fig. 3(b). They agree well with each other in the sense that the temperature rise of deformed sample decreases with the enhancement of deformation temperature. In the course of isothermal compression at 1080 K and $10\,s^{-1}$, the maximum temperature rise was calculated to be 83 K, whereas the actually measured sample surface temperature was about 25 K lower. It is clear that the sluggish dissipation of thermal energy created by plastic deformation is responsible for the flow localization accompanying shear banding.

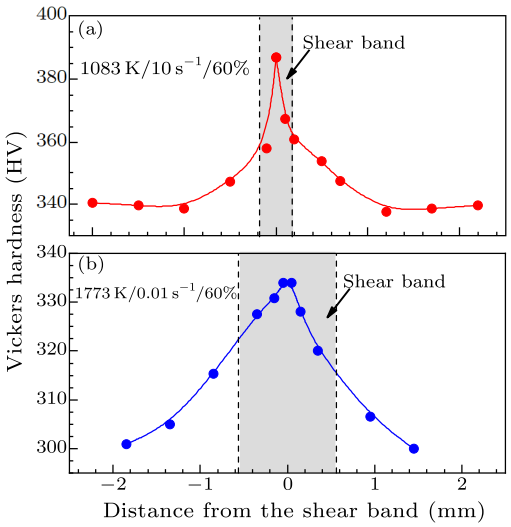

Fig. 5. Vickers hardness of shear band region and alloy matrix after deformed at (a) 1083 K/$10\,s^{-1}$ and (b) 1773 K/$0.01\,s^{-1}$.

Another sensitive parameter to characterize shear bands is the microhardness profile across relevant deformed zones. Figure 5 shows the Vickers hardness variations along the vertical axes of the two compressed samples with a true stain of 0.9 as seen in Figs. 4(a) and 4(b). Apparently, the hardness profile exhibits a maximum at shear band center. This may be reasonably attributed to the effects of grain refinement. In fact, the shear band region undergoes more plastic deformation and higher temperature than the sample matrix, both of which promote the dynamic recrystallization of initial martensitic structures. The maximum hardness of shear band is 387 HV (1 HV=1 N/mm^2=1 MPa) after deformed at 1083 K and $10\,s^{-1}$. It is reduced to 334 HV, if the deformation temperature rises to 1173 K and the strain rate falls to $0.01\,s^{-1}$. This indicates that a higher deformation temperature and a slower strain rate facilitate the coarsening of α phase grains, resulting in the decrease of microhardness.

In summary, we have investigated the dynamic formation mechanism of shear bands within isothermally compressed Ti-6Al-4V alloy with initial martensitic structures. The flow stress of this alloy decreases with the elevation of deformation temperature and the reduction of strain rate. The constitutive equation is derived for such a plastic deformation process, with the apparent activation energy being determined as 534.39 kJ/mol. The shear banding evolution is promoted by a higher deformation temperature and a lower strain rate. Although the moderate 0.01–$10\,s^{-1}$ strain rate regime corresponds to a nonadiabatic com-

pression event, the severe plastic deformation within shear band still induces a conspicuous temperature rise up to 83 K as predicted by theoretical analyses. The high temperature range of 1083–1173 K assisted with this concurrent temperature rise is sufficiently potent to initiate the dynamic recovery and recrystallization of the deformed martensitic structures. The experimentally detected microhardness profiles across shear bands lend further support to these conclusions.

The authors are very grateful to Professor N. Yan for her helpful discussion.

References

[1] Gourlay C M and Dahle A K 2007 *Nature* **445** 70
[2] Lewandowski J J and Greer A L 2006 *Nat. Mater.* **5** 15
[3] Quilichini A *et al.* 2016 *J. Geodyn.* **101** 109
[4] Hassani M, Lagogianni A E and Varnik F 2019 *Phys. Rev. Lett.* **123** 195502
[5] Sun B A *et al.* 2020 *Phys. Rev. B* **101** 224111
[6] Zheng J, Fu W J and Zhou L W 2013 *Chin. Phys. Lett.* **30** 094701
[7] Li S Z *et al.* 2016 *Appl. Phys. Lett.* **108** 022901
[8] Avila K E *et al.* 2020 *J. Appl. Phys.* **127** 115101
[9] Gillam B G *et al.* 2013 *J. Struct. Geol.* **54** 1
[10] Rolland Y and Rossi 2016 *J. Geodyn.* **101** 88
[11] Bi Z W *et al.* 2011 *Acta Phys. Sin.* **60** 034502 (in Chinese)
[12] Pan J *et al.* 2020 *Nature* **578** 559
[13] Wolf H, Koenig D and Triantafyllidis T 2003 *J. Struct. Geol.* **25** 1229
[14] Kroonblawd M P and Fried L E 2020 *Phys. Rev. Lett.* **124** 206002
[15] Sagapuram D *et al.* 2016 *Proc. R. Soc. A* **472** 20160167
[16] Park J M *et al.* 2008 *Appl. Phys. Lett.* **92** 091910
[17] Mara N A *et al.* 2010 *Appl. Phys. Lett.* **97** 021909
[18] Barbot A *et al.* 2020 *Phys. Rev. E* **101** 033001
[19] Ritter Y and Albe K 2012 *J. Appl. Phys.* **111** 103527
[20] Liu L F *et al.* 2011 *Chin. Phys. Lett.* **28** 036201
[21] Xue Q, Meyers M A and Nesterenko V F 2002 *Acta Mater.* **50** 575
[22] Zhang Z X *et al.* 2017 *J. Alloys Compd.* **718** 170
[23] Meier M L, Lesuer D R and Mukherjee A K 1991 *Mater. Sci. & Eng. A* **136** 71
[24] Shafaat M A, Omidvar H and Fallah B 2011 *Mater. & Des.* **32** 4689
[25] Liao S C and Duffy J 1998 *J. Mech. Phys. Solids* **46** 2201
[26] Rittel D, Landau P and Venkert A 2008 *Phys. Rev. Lett.* **101** 165501
[27] Kim Y *et al.* 2016 *J. Alloys Compd.* **676** 15
[28] Zhang X H, Zhao Y Q and Zeng W D 2019 *Mater. Lett.* **255** 126504
[29] Wang B F 2008 *J. Mater. Sci.* **43** 1576
[30] Nieto-Fuentes *et al.* 2019 *Phys. Rev. Lett.* **123** 255502